

Three-dimensional numerical and analytical study of horizontal group of square anchor plates in sand

Hicham Mokhbi, Mekki Mellas, Abdelhak Mabrouki, Jean-Michel Pereira

▶ **To cite this version:**

Hicham Mokhbi, Mekki Mellas, Abdelhak Mabrouki, Jean-Michel Pereira. Three-dimensional numerical and analytical study of horizontal group of square anchor plates in sand. Acta Geotechnica, 2018, 13 (1), pp.159-174. 10.1007/s11440-017-0557-x . hal-02882390

HAL Id: hal-02882390

https://enpc.hal.science/hal-02882390

Submitted on 26 Jun 2020

HAL is a multi-disciplinary open access archive for the deposit and dissemination of scientific research documents, whether they are published or not. The documents may come from teaching and research institutions in France or abroad, or from public or private research centers.

L'archive ouverte pluridisciplinaire **HAL**, est destinée au dépôt et à la diffusion de documents scientifiques de niveau recherche, publiés ou non, émanant des établissements d'enseignement et de recherche français ou étrangers, des laboratoires publics ou privés.

Three-dimensional numerical and analytical study of horizontal group of square anchor plates in sand

Hicham Mokhbi[1], Mekki Mellas[1], Abdelhak Mabrouki[1], Jean-Michel Pereira[2]

1 Civil Engineering Research Laboratory, University of Biskra, BP145 Biskra 07000, Algeria

2 Laboratoire NAVIER, École des Ponts Paris Tech, 6 et 8 avenue Blaise Pascal, 77420 Champs-sur-Marne, France

Abstract

In this paper, numerical and analytical methods are used to evaluate the ultimate pullout capacity of a group of square anchor plates in row or square configurations, installed horizontally in dense sand. The elasto-plastic numerical study of square anchor plates is carried out using three-dimensional finite-element analysis. The soil is modeled by an elasto-plastic model with a Mohr-Coulomb yield criterion. An analytical method based on a simplified three-dimensional failure mechanism is developed in this study. The interference effect is evaluated by group efficiency η, defined as the ratio of the ultimate pullout capacity of group of N anchor plates to that of a single isolated plate multiplied by number of plates. The variation of the group efficiency η was computed with respect to change in the spacing between plates. Results of the analyses show that the spacing between the plates, the internal friction angle of soil and the installation depth are the most important parameters influencing the group efficiency. New equations are developed in this study to evaluate the group efficiency of square anchor plates embedded horizontally in sand at shallow depth (H=4B). The results obtained by numerical and analytical solutions are in excellent agreement.

Keywords

Square anchor plate, group efficiency, finite elements, pullout capacity, sand, critical spacing.

1 Introduction

Anchor plates are lightweight structural elements, buried in the ground, used to resist the pullout forces acting on geotechnical structures such as submerged pipelines, offshore structures, retaining walls, and transmission towers. They may have various shapes (circular, helical, square, rectangular or strip). They are installed in the ground horizontally, vertically or in an inclined way. In the literature there are different theoretical, numerical and experimental works investigating the behavior of an isolated anchor plate and calculate its ultimate uplift capacity. One can cite Meyerhof and Adams (1968), Das (1978), Murray and Geddes (1987), Merifield and Sloan (2006), Hanna et al (2007), Khatri and Kumar (2009, 2010, 2011), Wang et al (2013), Bhattacharya and Kumar (2014), Mabrouki and Mellas (2014), Ardebili et al (2016), among others.

However, little information is available in the literature concerning the ultimate pullout capacity of a group of anchor plates. Table 1 presents some experimental, analytical and numerical works. Meyerhof and Adams (1968) proposed a theoretical relationship for calculating the ultimate pullout force of group of circular or rectangular foundations, buried in sand or in clay. Das and Yang (1987) have developed a physical model to evaluate the ultimate pullout force of a group of circular anchor plates buried in medium dense sand. They compared their results in terms of group efficiency with the theoretical solution of Meyerhof and Adams (1968), and they found that the ratio spacing/diameter (S/D) for a group efficiency η = 100%, for a given configuration, is approximately equal to the double of the one obtained theoretically. However, the general trend of the evolution of the group efficiency with respect to S/D ratio is similar to that of the theory.

In the present study, special attention was paid to the experimental model of Geddes and Murray (1996), to study the pullout force of a group of square anchor plates

53 embedded in a dense sand at a fixed depth, in different configurations. They reported
54 that, from a critical spacing ratio (S_{cr}/B = 2.9 for the test conditions used), the
55 maximum group efficiency is 100% and remains at that level when increasing the
56 spacing. This critical spacing is valid for all configurations and for a number of studied
57 anchor plates.
58 Abbad et al. (2013), have carried out an experimental study of the interaction of the
59 failure zones of square anchor plates installed at a depth of 5*B* in an analogical
60 environment formed by plastic granules. They used digital photographs at high
61 resolution processed by image correlation software to observe the displacement field
62 and plane strain of the analogical environment. They have reported that a minimum
63 spacing between axes of about seven times the width of the plate (7*B*) is necessary
64 for two neighboring anchor plates to act independently of each other.
65 In addition, other analytical studies of interferences within a group of strip anchor
66 plates, were established by Kumar and Kouzer (2008a), Kouzer and Kumar (2009a,
67 2009b), Merifield and Smith (2010), Ghosh and Kumari (2012), Kumar and Naskar
68 (2012), and Sahoo and Kumar (2014a, 2014b). These works fall within the limit
69 analysis framework, using the lower bound or the upper bound method. Table 1
70 shows the previous experimental and analytical works related to the study of the
71 interference of anchor plates in soils.
72 The main objective of this study is, on the one hand, to investigate numerically, using
73 three-dimensional non-linear finite element analysis, the group efficiency of square
74 anchor plates buried horizontally in a dense sand for several values of spacing/width
75 ratio (*S*/*B*). The effect of parameters like installation depth, internal friction angle of
76 soil, anchor roughness, and flow rule have been investigated numerically. On the
77 other hand, an additional objective is to develop an analytical solution of the group
78 efficiency of square anchor plates buried horizontally in the sand based on a failure

mechanism available in the literature, where a modification of the shape of the failure mechanism was introduced to simplify the calculation of the interference of failure mechanisms.

This study aims at highlighting recommendations concerning the calculation of pullout capacity of group of square anchor plates buried horizontally in a dense sand.

2 Numerical modeling

In this study, a three-dimensional numerical model was developed using the finite element method in Plaxis software, to investigate the ultimate uplift capacity of a group of square plate anchors. From previous experimental and theoretical studies on groups of plate anchors in soil (Table 1), the experimental work of Geddes and Murray (1996) seems the most appropriate as a reference for our work because it concerns the problem of square plates and contains the required data for numerical modeling. Geddes and Murray (1996) have performed a series of laboratory pullout tests on group of square plate anchors buried horizontally in dense sand. These tests were conducted in a steel box of size 1.28m × 1.22m × 0.89$m.$ The plate anchor have a square shape of width B = 50.8mm, buried at a fixed depth H = 203.2mm to give a ratio H/B = 4. Vertical uplift tests were carried out on two and five square plates in row configuration with constant spacing; and on groups of four square plates placed in a square configuration.

The symmetry of the problem enables to take a quarter model in all calculations as shown in Fig.1 which presents an example of a group of four anchor plates in square configuration. The dimensions of the numerical model adopted in all calculations (width, length and height) are constants according to the experimental model of Geddes and Murray (1996). The width of the model adopted is 0.61m and the height is 1$m;$ the square plate anchor have a width of B = 50$mm.$ It is verified that these

dimensions do not prevent the development of the failure mechanism for the large values of the spacing (*S*) considered in this study.

The small displacement assumption has been considered in all numerical analysis. The adopted soil model is a linear elastic-perfectly plastic model, obeying Mohr–Coulomb criterion with a non-associative flow rule. Referring to the study of Bolton (1986) on the strength and dilatancy of sands, the adopted dilation angle is $\psi' = \varphi' - 30°$. The anchor plate is modeled by plate elements with a linear elastic model. The values of soil parameters and elastic stiffness parameters of plate anchor used in this investigation are shown in Table 2. The soil parameters were taken from the Geddes and Murray (1996) study, and the elastic parameters of the material constituting the anchor plates were estimated from the literature studies (e.g., Hanna et al, 2011, Aghazadeh Ardebili et al, 2015, Ghosh, and Kumari, 2012).

Interface elements are used between soil and anchor plate elements to ensure sol-plate interaction. This type of interface elements allow for soil detachment. The interface behavior is defined by Mohr Coulomb criterion, with shear-strength characteristics calculated by the introduction of the strength reduction factor $R_{inter} \leq 1$, which gives the values of strength parameters of the interface element from the soil parameters by applying the strength reduction method suggested by Plaxis (Brinkgreve and Vermeer 2001) as follows:

$c_i' = R_{inter} c_{soil}'$,

$\tan \varphi_i' = R_{inter} \tan \varphi_{soil}' \leq \tan \varphi_{soil}'$

$\psi_i' = 0°$ for $R_{inter} < 1$, otherwise $\psi_i' = \psi_{soil}'$

where c_i', φ_i' and ψ_i' are the cohesion, the friction angle and the dilation angle of interface elements respectively.

A modified shear box test carried out by Geddes and Murray (1996) gave an interface friction angle of 10.6° for the sand studied in contact with polished steel plates, of the same kind as the anchors plates used in the uplift test. So for our case the strength reduction factor $R_{inter} = 0.19$.

Prescribed upwards displacements were applied at the nodes of anchor plates, and increase gradually until the stabilization of the resultant force which corresponds to the ultimate pullout force Q_u of the anchor plates group (Fig. 5). It should be noted that, using a displacement loading procedure, the parameters of the plate anchor do not affect the calculation results.

Before adopting the reference numerical model, several calculation tests were executed to check the influence of the mesh and the size of the model on calculation results, which allowed to suggest not only the use of a fine mesh in the vicinity of the anchor plate but also that the plate element itself must imperatively be discretized in 10 elements minimum on the x-y plane to get more accurate results. It was also verified that the boundaries of the numerical model based on the dimensions of the experimental model of Geddes and Murray (1996) have no effect on the value of the ultimate force obtained. It was finally checked that the values of the elastic parameters of soil have a negligible effect on the ultimate force computed by the numerical analysis.

3 Numerical results

The numerical finite element analyses that have been performed in this study concern the calculation of the ultimate pullout capacity of a group of square anchor plates, installed in row configuration: two (2 × 1), three (3 × 1), four (4 × 1) and five (5 × 1) square plates, or in square configuration: four (2 × 2) and nine (3 × 3) square plates, with a constant spacing *S* between the plates varying between 0 and 2.5*B.*

153 The group efficiency η was analyzed as a function of the spacing/width ratio (S/B) for
154 both row and square configurations for these relatively low values of S/B ratio. Then
155 the critical spacing S_{cr} between anchor plates was evaluated (corresponding to η =
156 100%). S_{cr} was defined as the distance from which each anchor plate acts
157 independently without interference between failure mechanisms (results discussed in
158 section 6).

159 **3. 1 Group of square anchor plates in row configuration**

160 Before starting the numerical analyses for group of plates, the pullout capacity of an
161 isolated square anchor plate was calculated. The evolution of pullout load with
162 displacement was plotted in Fig. 5 (bottom curve). The failure mechanism of this
163 isolated square anchor plate can be observed in Fig. 2. Its shape can be considered
164 as a truncated cone with slightly curved failure planes near the ground surface.
165 In order to investigate the influence of elastic parameters of soil on the ultimate
166 pullout capacity, the case of a single square anchor plate are analysed with different
167 values of Young's modulus (E = 10, 30 and 60 MPa). Fig. 3 shows the results
168 obtained for H/B = 4 and H/B = 6; It can be observed that the values of the elastic
169 parameters have a small effect on the ultimate pullout capacity. However, for great
170 values of E the ultimate load is reached for a smaller displacement.
171 Fig. 4 illustrates a group of square anchor plates of width B, installed in row
172 configuration with a similar spacing S. The total line length is noted L.
173 Fig. 5 shows the results of the ultimate pullout load as a function of displacement for
174 a group of two square anchor plates with different values of S/B ratio varying from 0
175 to 2, indicating that the force Q_u increases with increasing spacing between the two
176 anchor plates. This trend illustrates the presence of group effects on the ultimate
177 pullout capacity. Fig. 6 presents the total displacements obtained in the case of two

anchor plates with a ratio of *S*/*B* = 2. It also shows the interference of the failure mechanisms of the two adjacent plates.

The group efficiency *η* was calculated by the following conventional relation (Das (1990), Geddes and Murray (1996), Emirler et al (2015)):

$$\eta\,(\%) = \frac{Ultimate\ load\ of\ group\ of\ N\ anchors\ \times 100}{N\ \times ultimate\ load\ of\ an\ isolated\ anchor} \qquad (1)$$

with *N* the total number of anchor plates.

Fig. 7 shows the evolution of the group efficiency of square anchor plates in row configuration (two (2 × 1), three (3 × 1), four (4 × 1) and five (5 × 1)) with the spacing/width ratio (*S*/*B*). In the same figure are plotted the experimental results obtained by Geddes and Murray (1996) in the case of two (2 × 1) and five (5 × 1) plates.

The numerical results show that the evolution of the group efficiency as a function of (*S/B*) ratio is perfectly linear, and may be fitted with Equations (2), (3), (4) and (5) for configurations (2×1), (3×1), (4×1) and (5×1) respectively. For the case of two plates (2 x 1), the group efficiency *η* increases linearly from 61% for *S/B* = 0 corresponding to a rectangular plate *L/B* = 2 to 78% for *S/B* = 2. For the case of three plates (3 x 1), *η* increase linearly from 48% for *S/B* = 0 corresponding to a rectangular plate *L/B* = 3 to 77% for *S/B* = 2.5. For the case of four plates (4 x 1), *η* increase linearly from 41% for *S/B* = 0 corresponding to a rectangular plate *L/B* = 4 to 74% for *S/B* = 2.5. For five plates (5 x 1), *η* increase also linearly from 37% for *S/B* = 0 corresponding to a rectangular plate *L/B*=5 to 72% for *S/B* = 2.5.

$$\eta_{2\times1}(\%) = 8.537\frac{S}{B} + 60.96 \qquad (2)$$

$$\eta_{3\times1}(\%) = 11.45\frac{S}{B} + 48.13 \qquad (3)$$

$$\eta_{4\times1}(\%) = 13.25\frac{S}{B} + 40.68 \quad (4)$$

$$\eta_{5\times1}(\%) = 13.85\frac{S}{B} + 36.94 \quad (5)$$

198 The values of group efficiency obtained experimentally by Geddes and Murray (1996)
199 are larger than the numerical results, except for the first point (*S/B* = 0) which is
200 superimposed to the numerical point in both cases (2 x 1) and (5 x 1). For the case of
201 five plates (5 x 1), the difference between the experimental and numerical results
202 increases with the increase of *S/B* ratio, and remains nearly constant around 10% for
203 the case of two plates (2 x 1). However, the experimental results also show a linear
204 trend from the second point corresponding to *S/B* = 0.25 or *S/B* = 0.5. On this point,
205 Geddes and Murray (1996) reported that the relationship between *S*/*B and* the group
206 efficiency demonstrates an initial perturbation followed by a linear trend.
207 The group efficiency obtained experimentally varies from about 59% for *S*/*B* = 0 to
208 about 90% for *S/B* = 2 in the case of two plates (2 x 1). For five plates, *η* varies from
209 about 37% for *S/B* = 0 to about 71% for *S*/*B* =2.5.
210 From these results in row configuration, we can conclude that the group efficiency of
211 *N* plates is lower than that of (*N* - 1) plates for the same spacing *S*, and this
212 difference of efficiency decreases when the spacing/width ratio (*S/B*) increases.

213 **3. 2 Group efficiency of square plates in square configuration**

214 For a square configuration, Fig. 8 illustrates the two cases studied: groups of four (2
215 × 2) and nine (3 × 3) square anchor plates. Fig. 9 presents the total displacements
216 obtained in the case of nine anchor plates with a ratio of *S*/*B* = 2. It also shows the
217 interference between failure mechanisms of plates.
218 Fig. 10 shows the numerical results of these cases in comparison with the
219 experimental results obtained by Geddes and Murray (1996). The numerical results

show that η increases linearly as a function of S/B ratio, following the two Equations (6) and (7) for the case of four (2 × 2) and nine (3 × 3) plates respectively. For the case of four plates (2 × 2), η evolves linearly from 34% for S = 0 (corresponding to a single square plate of width equal to 2B), to 67% for S/B = 2.5. For the case of nine (3 × 3) plates, η increase from 20% for S = 0 (corresponding to the case of a single square plate of width equal to 3B), to 52% for S/B = 2.5.

The experimental results of Geddes and Murray (1996) for four square plates (2 x 2), shows that η evolves almost linearly with S/B ratio, from 34% for S = 0 to approximately 85% for S/B = 2.5. However, the experimental values of η are larger than the numerical values except for the case of S/B = 0 where the values of η are equal, then the difference between the numerical and experimental values of η increases gradually with the increase of S/B.

$$\eta_{2\times2}(\%) = 13.39\frac{S}{B} + 33.48 \quad (6)$$

$$\eta_{3\times3}(\%) = 12.92\frac{S}{B} + 19.81 \quad (7)$$

It is also remarkable that for any given value for S/B ratio, the group efficiency of four square anchor plates installed in square configuration is lower than in the case of four square anchor plates installed in row configuration. The reason is that in square configuration, the failure mechanism of each of the four plates interferes with that of the two or three other plates. In row configuration, the failure mechanism of each of the intermediate plates interferes with that of the two nearby plates, and the failure mechanism of each of the edge plates interferes only with that of a single plate. This difference of group efficiency between a row and square configuration becomes larger with the increase of the number of anchor plates.

3. 3 Load factors

The previous numerical results highlighted that the group efficiency of a group of square anchor plates installed horizontally in sand, in row or square configuration, evolves linearly with *S/B* ratio. In order to establish a general equation of the group efficiency of *N* anchor plates, the previous data of group efficiency, for row and square configurations, were redrawn in terms of load factor F_L versus *L/B* ratio. According to Geddes and Murray (1996), the following relationship holds:

$$\frac{L}{B} = n + (n-1)\frac{S}{B} \tag{8}$$

with n the number of plate per row,

$$F_L = \frac{Ultimate\ load\ of\ N\ plates}{Ultimate\ load\ of\ a\ single\ isolated\ plate} \tag{9}$$

or

$$F_L = \eta \times N/100 \tag{10}$$

Fig. 11 presents the variation of the load factor according to *L/B* ratio for all row configurations studied previously. The load factor evolves linearly with *L/B* ratio for two, three, four and five anchor plates in row configuration. This linear relation is best fitted by the following equation:

$$F_L = 0.182\ (L/B) + 0.866 \tag{11}$$

From Equations (8), (10) and (11), we can write a general relation (12) of the group efficiency of *n* square anchor plates installed horizontally in the sand in row configuration (*n* = *N*). Nevertheless, this relation is valid only for the geotechnical and geometrical characteristics chosen in this study.

$$\eta_{n\times 1}(\%) = \frac{18.2}{n}\left(n + (n-1)\frac{S}{B}\right) + \frac{86.6}{n} \quad (12)$$

Besides, by drawing the curve of the load factor according to *L/B* ratio for the case of four and nine anchor plates in square configuration (Fig. 12), a global linear relation of the evolution of the load factor is obtained:

$$F_L = 0.561\ (L/B) + 0.167 \quad (13)$$

So, from equations (8), (10), and (13) we can write the general relation (14) of the group efficiency of ($N = n \times n$) square anchor plates installed horizontally in the sand in square configuration, which also is valid only for the geotechnical and geometrical characteristics considered in this study:

$$\eta_{n\times n}(\%) = \frac{56.1}{n^2}\left(n + (n-1)\frac{S}{B}\right) + \frac{16.7}{n^2} \quad (14)$$

4 Parametric study

The previous numerical calculations have established the general Equations (12) and (14) of the group efficiency for row and square configurations respectively. These relations concern the case of $H/B = 4$, and involve the following variables: number of anchor plates, spacing between anchor plates and width of plates. However, a parametric study is needed to verify the influence of various parameters on the obtained results. To this aim, a numerical parametric study was carried out on a group of two square anchor plates, studying the influence of installation depth, internal friction angle of soil, flow rule and roughness of anchors.

4.1 Influence of installation depth

To study the influence of installation depth on the group efficiency, the ultimate pullout capacity of two square anchor plates was calculated for a depth/width ratio

H/B = 2 and *H/B* = 6. Then the group efficiency was calculated and compared with those obtained for the reference model (*H/B* = 4) as shown in Fig. 13.

Fig. 13 shows that the group efficiency for a given spacing decreases when the *H/B* ratio increases. Indeed, the critical spacing (S_{cr}) increases with depth (*H*). This is explained by the relationship between the critical spacing and the installation depth theoretically estimated by $S_{cr} = 2H \tan\theta$, with θ is the inclination angle of the failure plane with the vertical as shown in Fig. 21.

In previous studies, the installation depth has also an influence on the shape of failure mechanisms. There is a critical embedment ratio which presents the transition between shallow anchor behaviour and deep anchor behaviour. Meyerhof (1973) proposed a critical embedment ratio *H/B* = 4 for square anchors in loose sand, and it increases up to about 8 in dense sand. Also, Das (1983) proposed an empirical correlation for the critical embedment ratio for square anchor plates in the form $\mathrm{H/B} = 5.5 + 0.166(\varphi - 30)$, (for 30° ≤ *φ* ≤ 45°).

Fig. 14 shows the total displacement for the case of two square anchor plates embedded at different depths with *H/B* varying from 4 to 10. The mechanisms are depicted by the contours of finite element displacement; where the same scale was used to present the displacement field for all embedment ratio values. It is seen that from embedment ratio *H/B* ≥ 8*H* the failure mechanism begins to develop locally. From the present study, the embedment ratio *H/B* = 8 can be considered as the critical embedment ratio.

4.2 Influence of internal friction angle

The reference numerical model was studied with an internal friction angle *φ′* = 43.6°. However, to study the influence of this parameter on the group efficiency, other numerical calculations were performed, also for a group of two square anchor plates,

with other values of the internal angle friction φ' = 30° and φ' = 20°. For these values of φ', the adopted dilation angle is equal to zero. The results of numerical calculations are presented in Fig. 15 showing a little influence compared to the depth parameter on the group efficiency. η increases by 8% when φ' decreases from 43.6° to 20°. This influence can be explained by the relation of the failure mechanism with the internal friction angle. Some authors such as Clemence and Veesaert (1977) found that the inclination angle of the failure plane with the vertical is equal to the half of the internal friction angle of soil. Murray and Geddes (1987), and Merifield et al (2006) found that this inclination angle is equal to the internal friction angle. So, when φ' decreases the interference between failure mechanisms decreases and η increases.

4.3 Influence of dilation angle

To study the influence of the flow rule on the group efficiency, other numerical calculations were established for the case of two square anchor plates. An associated flow rule ($\psi' = \varphi'$) was considered, and the obtained results of the group efficiency were compared with the results of the reference case calculated with a non-associated flow rule ($\psi' = \varphi' - 30°$). This comparison is presented in Fig. 16 and shows an almost negligible effect on the group efficiency according to *S/B* ratio. However, it should be noted that there is a significant influence of the dilation angle on the value of the ultimate pullout capacity, which is overestimated with an associated flow rule (up to 38%).

4.4 Influence of anchor roughness

In the reference model, the interface between the soil and the anchor plate was determined by using a strength reduction factor $R_{inter} = 0.19$. To study the influence of anchor roughness on the group efficiency, other calculations were performed for a group of two square anchor plates, with the following values of the strength reduction

factor $R_{inter} = 0.33;\ 0.5;\ 0.75$ and 1. The results of group efficiency are presented in Fig. 17, which show that there is a very little influence on the values of group efficiency. This is can be explained by the shape of failure mechanism, where there is no significant mobilization of shearing resistance between the soil and the anchor plate during the pullout action. Rowe and Davis (1982b) found that the roughness has a negligible effect on the capacity of horizontal anchors at all depths, but significantly increases that of shallow vertical anchors (*H*/*B* < 3). For this latter case, they found that the effect of roughness is increased further if the soil is dilatant.

5 Analytical solution for *n* square anchor plates in row configuration

5.1 Isolated anchor plate

Murray and Geddes (1987) have developed a failure mechanism using the upper bound limit analysis, for a rectangular anchor plate installed horizontally in a frictional soil, and subjected to a vertical pullout loading. This failure mechanism consists in a failure plane inclined at an angle φ' to the vertical at the edge of the plate. At the corners the failure mechanism consists in a portion of a circular cone. They have obtained the following expression for the break-out factor N_γ *:*

$$N_\gamma = 1 + \frac{H}{B}\tan\varphi'\left(1 + \frac{B}{L} + \frac{\pi}{3}\frac{H}{L}\tan\varphi'\right) \qquad (15)$$

To simplify the analytical calculation of the interference of a group of square anchor plates, the portion of a circular cone at the corners were replaced by a vertical pyramid. The inclination angle (θ) of the failure plane with the vertical was adopted using this empirical relation $\theta = 0.785\,\varphi'^{1.1}$ with φ' is expressed in degree (Fig. 18). Following the theory of Mors (1959), the ultimate pullout capacity is assumed equal to the weight of soil located within the failure mechanism; and the frictional resistance acting along the failure surface was ignored. Ilamparuthi et al. (2002) have reported

that the method of Mors (1959) is usually conservative for shallow anchors but overpredicts pullout capacity for deeper anchors. This method was also followed by Ganesh and Sahoo (2015) to estimate the ultimate uplift resistance of circular anchor plate. They reported that the frictional resistance acting along the failure surface can be ignored, conservatively, for the case of shallow anchors. It is worthwhile noting that the present study considers the anchor plates embedded at shallow depth (*H=4B*).

The break-out factor of this modified failure mechanism is given in equation (16) (see details in appendix A). The values of N_γ obtained by this expression (16) give a very satisfactory agreement with the upper bound results obtained by Murray and Geddes (1987), and the lower bound results obtained by Merifield et al. (2006) as shown in Fig. 19.

$$N_{\gamma\ isolated} = 1 + 2\frac{H}{B}\tan\theta + \frac{2}{3}\left(\frac{H}{B}\right)^2 \tan^2\theta \qquad (16)$$

In order to examine the effect of soil strength along the failure surface on the ultimate pullout capacity, numerical analyses were carried out by modeling a full-scale square plate (B = 1m) with embedment ratio H/B varying from 1 to 5, and ϕ' = 20°, 30° and 40° by considering an associative flow rule. The model adopted in these numerical analyses, has a depth of 10 m and extends 6 m beyond the planes of symmetry.

The values of the break-out factor Nɣ obtained from the present numerical analyses were compared with those calculated with the expression (16) as shown in Fig. 20. The comparison shows that the values of Nɣ obtained by the expression (16) are slightly smaller than the numerical values. Consequently, when the soil strength along the failure surface is ignored, the result always errs on the safe side; it underestimates the ultimate pullout capacity. However, the relative error from the use

of this assumption varies between 3% and 17%, and it increases slightly with the increase in embedment ratio.

5.2 Two square anchor plates

For a group of two square anchor plates spaced by $S < 2H\tan\theta$, the ultimate pullout capacity of each anchor plate is simply equal to the weight of the soil located within the failure mechanism (defined by points a, b, c, d, e for the left anchor, as shown in Fig. 21). The break-out factor corresponding to this volume is noted by $N_{\gamma end}$ and given by: (see details in appendix B)

$$N_{\gamma\ end} = 1 + \frac{1}{3}\left(\frac{H}{B}\right)^2 (\tan\theta)^2 + \frac{1}{2}\left(3 + \frac{S}{B}\right)\frac{H}{B}\tan\theta + \frac{1}{8}\frac{S}{H}\frac{S}{B}\left(\frac{1}{3}\frac{S}{B} - 1\right)\cot\theta - \frac{1}{4}\left(\frac{S}{B}\right)^2 + \frac{1}{2}\frac{S}{B} \quad (17)$$

The group efficiency of two anchor plates noted $\eta_{2\times1}$ can be calculated with the following relationship:

$$\eta_{2\times1}(\%) = \frac{N_{\gamma\ end}}{N_{\gamma\ isolated}} \times 100 \quad (18)$$

Fig. 22 shows the group efficiency of two anchor plates as a function of *S/B* ratio, as predict by Equation (18), in comparison with our numerical results and the experimental results obtained by Geddes and Murray (1996). Additional calculations were performed using Plaxis software for (*S/B* = 4.5, 5 and 5.5).

In general, it can be noted that the analytical results are in good agreement with numerical results. However, the experimental results obtained by Geddes and Murray (1996) show higher values than both analytical and numerical results.

5.3 *n* square anchor plates in row configuration

For a group of *n* square anchor plates spaced by $S < 2H\tan\theta$, the ultimate pullout capacity of an intermediate anchor plate is simply equal to the weight of the soil located within the failure mechanism defined by points a, b, c, d, e, f as shown in Fig.

394 23. The break-out factor corresponding to this volume is noted $N_{\gamma\ inter}$ and given by:
395 (see details in appendix C)

$$N_{\gamma\ inter} = 1 + \left(1 + \frac{S}{B}\right)\frac{H}{B}\tan\theta - \frac{1}{3}\frac{S}{B}\frac{S}{H}\left(\frac{1}{4}\frac{S}{B} - 1\right)\cot\theta - \frac{1}{2}\left(\frac{S}{B}\right)^2 + \frac{S}{B} \quad (19)$$

396 In this case, the group efficiency of *n* anchor plates can be calculated with the
397 following expression:

$$\eta_{n\times 1}(\%) = \frac{(n-2)N_{\gamma\ inter} + 2N_{\gamma\ end}}{n\ N_{\gamma\ isolated}} \times 100 \quad (20)$$

398 Fig. 24 shows the comparison of numerical, analytical and experimental results of the
399 group efficiency of five square anchor plates in row configuration. These results
400 correspond to small values of the spacing between the plates ($0 < S/B < 2$). A good
401 agreement is observed between the analytical results and the numerical results.

402 **6 Critical spacing for two square anchor plates**

403 Based on previous analytical and numerical results, we can determine the critical
404 spacing for which two anchor plates (placed at a depth *H* = 4*B* in this study) act
405 independently, so that the group efficiency is equal to 100%.

406 The numerical results highlight that a critical spacing of $S_{cr} = 5.5B$, is necessary for a
407 group of anchor plates installed in linear configuration to obtain a group efficiency of
408 100%. The critical spacing obtained by equation (12) is $S_{cr} = 4.24B$. However, the
409 additional calculations performed for verification by Plaxis software have given a
410 group efficiency *η* = 97% for *S/B* = 4.24 as shown in Fig. 22.

411 The analytical calculation have given results very similar to the numerical results
412 especially for small values of *S/B* (0 < *S/B* <2). However the critical spacing obtained
413 analytically for *η* = 100% is $S_{cr} = 7.5B$ as shown in Fig. 22. Despite this remarkable
414 difference between the critical spacing obtained by the numerical calculation and that
415 obtained by an analytical solution, the relative error between them is of the order of

3.86% for a critical spacing $S_{cr} = 5.5B$. On the other hand, Geddes and Murray (1996) found in their experimental study a critical spacing of $S_{cr} = 2.9B$.

In addition, there is little information in the literature on the critical spacing with the exception of the works presented in Table 3. It is important to examine the experimental study of Abbad et al. (2013) on the interference of square anchor plates (B = 5 cm) installed at a depth of H = 5B in a material made of plastic grains with a diameter of 1 mm. The analogical medium has a relative density of Dr = 96% (e_{min} = 0.302, e_{max} = 0.855), with a dry unit weight of γ_d = 14,6 kN/m^3, a null cohesion and an initial friction angle φ = 39°. Using high resolution digital pictures, they have found that a minimum spacing $S_{cr} = 6B$, is necessary for two anchor plates to act independently.

Das and Yang (1987) has developed an experimental study for circular anchor plates embedded in a sand with φ' = 37°, he found a critical spacing $S_{cr} = 3D$. For the same characteristics, Meyerhof and Adams (1986) found $S_{cr} = 1.8D$.

The difference observed between the critical spacing obtained numerically and that obtained analytically is attributed to the shape of the failure mechanism. Analytical calculations consider an associated soil ($\psi' = \varphi'$), which overestimates the ultimate pullout capacity and provides a larger failure mechanism, thus requiring a bigger critical spacing. Inversely, the numerical calculations, account for a non-associated flow rule ($\psi' = \varphi' - 30°$) which induce a narrower failure mechanism thus requiring a smaller critical spacing.

7 Conclusion

The ultimate pullout capacity of a group of square anchor plates in row or square configurations was calculated, using three-dimensional finite elements analyses. The square anchor plates were installed horizontally in dense sand and pulled vertically. The soil is characterized by the Mohr-Coulomb yield criterion and non-associative

flow rule. In this study, a simple three-dimensional failure mechanism has been proposed to evaluate the anchor break-out factor and the group efficiency. The evolution of the group efficiency η with the spacing/width ratio (S/B) was analyzed and compared with results available in the literature.

In this paper, a numerical parametric study was conducted on a group of two square anchor plates to identify the most influential parameters on the group efficiency. This parametric study revealed that the group efficiency η increases considerably with the decrease of the internal friction angle φ', and the installation depth H. On the other hand, η is slightly influenced by the anchor roughness and the choice of an associative flow rule. Nevertheless, it is worthwhile noting that the associative flow rule highly overestimates the value of the ultimate pullout capacity. The group efficiency of N square anchor plates installed in row configuration is greater than that of N square anchor plates installed in square configuration.

The comparison of the numerical results with analytical solutions confirmed that the proposed failure mechanism predict a group efficiency values in good agreement with those obtained by elasto-plastic analyses. New equations are developed in this study to evaluate the group efficiency of shallow square anchor plates (H=4B). The group efficiency evolves linearly with S/B ratio, until a critical value of the spacing between plates beyond which the anchor plates act independently. For this critical spacing, the ultimate pullout load of the group arrives at its maximal value and remains stable, in spite of the increase of the spacing. The value of critical spacing for which the two square anchor plates can be assumed isolated, as predicted by the present numerical computations, is approximately 5.5 times the width of the plate B.

References

1. Abbad, H., Meghachou, M., Dekar, C., and Daoud, S. M. (2013). Interaction of Rupture Zones of Adjacent Anchor Plates in an Analogical Medium. *ETASR - Engineering, Technology & Applied Science Research*, 3(6):562-565.
2. Ardebili ZA, Gabr MA, Rahman MS (2016). Uplift Capacity of Plate Anchors in Saturated Clays: Analyses with Different Constitutive Models. *International Journal of Geomechanics*, *16*(2), 4015053.
3. Bhattacharya, P., and Kumar, J. (2014). Vertical pullout capacity of horizontal anchor plates in the presence of seismic and seepage forces. *Geomechanics and Geoengineering*, 9(4):294-302.
4. Bolton, M. D. (1986). The strength and dilatancy of sands. *Géotechnique* 36(1):65-78
5. Brinkgreve, R.B.J., and Vermeer, P.A. (2001). Plaxis Finite Element Code for Soil and Rock Analyses, Version 1, BALKEMA.
6. Clemence SP, Veesaert CJ (1977) Dynamic pullout resistance of anchors in sand. In: roceedings of the International Symposium on Soil-Structure Interaction, Roorkee, India, pp 389–397
7. Das B. M., Yang Jin-Kaun (1987), Uplift Capacity of Model Group Anchors in Sand. Foundations for Transmission Line Towers, *Geotechnical Special Publication* No. 8, ASCE
8. Das, B. M. (1978). Model tests for uplift capacity of foundations in clay. *Soils and Found.* 18(2):17-24.
9. Das, B.M., (1983). A procedure for estimation of uplift capacity of rough piles. *Soils and Found*., Japan, 23(3):122-126.
10. Das, B. M. (1990). *Earth Anchors. Developments in Geotechnical Engineering*, 50: 1-241.

11. Emirler, B. Bildik, S., and Laman, M. (2015). Numerical Investigation of Group Anchors. *IFCEE 2015 © ASCE* 279–288.
12. Ganesh, R., and Sahoo, J. P. (2015). Influence of ground water on the ultimate uplift resistance of circular plate anchors. *50th Indian geotechnical Conference 17th - 19th December 2015, Pune, Maharashtra, India.*
13. Geddes, J.D., and Murray, E.J. (1996). Plate anchor groups pulled vertically in sand. *J. Geotech. Engrg.,* ASCE 122(7):509–516.
14. Ghosh, P., and Kumari, R. (2012) Seismic interference of two nearby horizontal strip anchors in layered soil. *Nat Hazards,* 63:789–804
15. Hanna, A., Ayadat, T., and Sabry, M. (2007). Pullout resistance of single vertical shallow helical and plate anchors in sand. *Geotechnical and Geological Engineering*, *25*(5):559–573.
16. Hanna A, Rahman F, Ayadat T (2011) Passive earth pressure on embedded vertical plate anchors in sand. Acta Geotechnica, 6(1), 21–29.
17. Ilamparuthi, K., Dickin, E. A., and Muthukrisnaiah, K. (2002). Experimental investigation of the uplift behaviour of circular plate anchors embedded in sand. *Can. Geotech. J.*, 39: 648–664.
18. Khatri, V. N., and Kumar, J. (2009). Vertical uplift resistance of circular plate anchors in clays under undrained condition. *Computers and Geotechnics*, 36(8):1352–1359.
19. Khatri, V. N., and Kumar, J. (2010). Stability of an unsupported vertical circular excavation in clays under undrained condition. *Computers and Geotechnics*, 37(3):419–424.
20. Khatri, V. N., and Kumar, J. (2011). Effect of anchor width on pullout capacity of strip anchors in sand. *Canadian Geotechnical Journal*, 48(3):511–517.

21. Kouzer, K. M., and Kumar, J. (2009a). Vertical uplift capacity of two interfering horizontal anchors in sand using an upper bound limit analysis. *Computers and Geotechnics,* 36(6):1084–1089.
22. Kouzer, K. M., and Kumar, J. (2009b). Vertical uplift capacity of equally spaced horizontal strip anchors in sand. *International Journal of Geomechanics,* 9(5):230-236.
23. Kumar, J., and Kouzer, K.M. (2008a). Vertical uplift capacity of a group of shallow horizontal anchors in sand. *Géotechnique,* 58(10):821–823.
24. Kumar, J., and Naskar, T. (2012). Vertical uplift capacity of a group of two coaxial anchors in a general c–φ soil. *Canadian Geotechnical Journal,* 49(3): 367–373.
25. Mabrouki, A., and Mellas, M. (2014). Étude tridimensionnelle de la capacité ultime des plaques d'ancrage dans un sol frottant. *Courrier Du Savoir*, (18):15–19.
26. Merifield, R.S., and Sloan, S.W. (2006). The ultimate pullout capacity of anchors in frictional soils. *Can. Geotech. J.* 43(8):852–868.
27. Merifield R S, Lyamin A V, Sloan S W (2006) Three dimensional lower bound solutions for the stability of plate anchors in sand. Géotechnique 56(2):123–132.
28. Merifield, R.S and Smith, C.C. (2010). The ultimate uplift capacity of multi-plate strip anchors in undrained clay. *Computers and Geotechnics* 37:504–514
29. Meyerhof, G. G. and Adams, J. I. (1968). The ultimate uplift capacity of foundations. *Canadian Geotechnical Journal* 5(4):225–244.
30. Meyerhof, G. G. (1973) “Uplift resistance of inclined anchors and piles” Proc. of VIII International Conference on Soil mechanics and Foundation Engineering, Moscow, USSR, 2, 1, 167-172.

31. Mors, H. (1959). The behaviour of mast foundations subject to tensile forces. *Bautechnik*, 10: 367–378.
32. Murray, E. J., and Geddes, J. D. (1987). Uplift of anchor plates in sand. *J. Geotech. Engrg.*, 113(3):202–215.
33. Rowe, R. K. and Davis, E. H. (1982b). The behaviour of anchor plates in sand. *Géotechnique,* 32(1):25–41.
34. Sahoo, J. P., and Kumar, J. (2014a). Vertical uplift resistance of two closely spaced horizontal strip anchors embedded in cohesive – frictional weightless medium. *Can. Geotech. J.,* 51:223–230.
35. Sahoo, J. P., and Kumar, J. (2014b). Vertical uplift resistance of two interfering horizontal anchors in clay. *J. Geotech. Geoenviron. Eng.,* 140(4):06013007
36. Wang, D., Merifield, R.S., and Gaudin, C. (2013). Uplift behaviour of helical anchors in clay. *Can. Geotech. J.* 50:575-584.

Appendix A: Analytical solution of break-out factor $N_{\gamma\,isolated}$ for an isolated square anchor plate

Volumes of the portions 1, 2 and 3 shown in Fig. 25:

$$V_1 = B^2 H \tag{21}$$

$$V_2 = 0.5BH^2 \tan\theta \tag{22}$$

$$V_3 = \frac{1}{6} H^3 \tan^2\theta \tag{23}$$

The ultimate pullout load Q_u is equal to the weight of the soil located within the failure mechanism:

$$Q_u = \gamma(V_1 + 4V_2 + 4V_3) \tag{24}$$

Using Equations 21, 22 and 23, we finally get:

$$Q_u = B^2\gamma H + 2\gamma H^2 B\tan\theta + \frac{2}{3}\gamma H^3\tan^2\theta \quad (25)$$

564 By definition, the ultimate pullout capacity q_u:

$$q_u = \frac{Q_u}{A} = \frac{Q_u}{B^2} \quad (26)$$

$$q_u = \gamma H\left(1 + 2\frac{H}{B}\tan\theta + \frac{2}{3}\left(\frac{H}{B}\right)^2\tan^2\theta\right) \quad (27)$$

565 By convention, q_u is also given by:

$$q_u = \gamma H N_\gamma \quad (28)$$

566 So that the break-out factor N_γ for an isolated square plate anchor is:

$$\boldsymbol{N_{\gamma\,isolated} = 1 + 2\frac{H}{B}\tan\theta + \frac{2}{3}\left(\frac{H}{B}\right)^2\tan^2\theta} \quad (29)$$

567 **Appendix B: Analytical solution of break-out factor $N_{\gamma\,end}$ for a square anchor**

568 **plate located at an end**

569 For two or n square anchor plates with $S < 2H\tan\theta$, the ultimate pullout load of one

570 anchor plate at the end is equal to the weight of the soil located within its failure

571 mechanism defined by points a, b, c, d, e shown in Fig. 21.

572 Volumes of the portions 4 and 5 shown in Fig. 26:

$$V_4 = \frac{1}{2}(2H\tan\theta - S)\left(H - \frac{S}{2}\cot\theta\right)B \quad (30)$$

$$V_4 = BH^2\tan\theta + B\frac{S^2}{4}\cot\theta - BSH \quad (31)$$

$$V_5 = \frac{1}{3}\times\frac{1}{2}\left(\sqrt{2}H\tan\theta - S\frac{\sqrt{2}}{2}\right)^2\left(H - \frac{S}{2}\cot\theta\right) \quad (32)$$

$$V_5 = \frac{1}{3}H^3\tan^2\theta - \frac{1}{2}SH^2\tan\theta - \frac{S^3}{24}\cot\theta + \frac{1}{4}S^2H \quad (33)$$

573 The volume *V* corresponding to points a, b, c, d, e shown in Fig.16 is equal to:

$$V = V_T - \frac{1}{2}V_4 - 2\left(\frac{1}{2}V_5\right) = V_T - \frac{V_1}{2} - V_5 \quad (34)$$

574 Where V_T is the total volume of soil located within the failure mechanism for an
575 isolated square anchor plate.
576 So:

$$V = B^2H + \frac{3}{2}H^2B\tan\theta + \frac{1}{3}H^3\tan^2\theta - \frac{1}{8}BS^2\cot\theta + \frac{1}{2}BSH + \frac{1}{2}SH^2\tan\theta + \frac{1}{24}S^3\cot\theta - \frac{1}{4}S^2H \quad (35)$$

577 The ultimate pullout capacity of anchor plate located at the end is then:

$$q_{u\,end} = \frac{Q_{u\,end}}{A} = \frac{Q_{u\,end}}{B^2} = \frac{\gamma \times V}{B^2} \quad (36)$$

578 Using Equation 35, we get:

$$q_{u\,end} = \gamma H\left(1 + \frac{3}{2}\left(\frac{H}{B}\right)\tan\theta + \frac{1}{3}\left(\frac{H}{B}\right)^2(\tan\theta)^2 - \frac{1}{8}\left(\frac{S}{B}\right)\left(\frac{S}{H}\right)\cot\theta + \frac{1}{2}\left(\frac{S}{B}\right) + \frac{1}{2}\left(\frac{S}{B}\right)\left(\frac{H}{B}\right)\tan\theta + \frac{1}{24}\left(\frac{S}{B}\right)^2\left(\frac{S}{H}\right)\cot\theta - \frac{1}{4}\left(\frac{S}{B}\right)^2\right) \quad (37)$$

579 Since:

$$q_{u\,end} = \gamma H N_{\gamma\,end} \quad (38)$$

580 We finally obtained $N_{\gamma\,end}$

$$N_{\gamma\,end} = 1 + \frac{1}{3}\left(\frac{H}{B}\right)^2(\tan\theta)^2 + \frac{1}{2}\left(3 + \frac{S}{B}\right)\frac{H}{B}\tan\theta + \frac{1}{8}\frac{S}{H}\frac{S}{B}\left(\frac{1}{3}\frac{S}{B} - 1\right)\cot\theta - \frac{1}{4}\left(\frac{S}{B}\right)^2 + \frac{1}{2}\frac{S}{B} \quad (39)$$

581

582 **Appendix C: Analytical solution of break-out factor $N_{\gamma\,\mathrm{inter}}$ for an intermediate**
583 **square anchor plate**

584 For *n* square anchor plates in row configuration with $S < 2H\tan\theta$, the ultimate pullout
585 load of an intermediate anchor plate is equal to the weight of the soil located within
586 its failure mechanism defined by points a, b, c, d, e, f as shown in Fig. 23. The break-
587 out factor corresponding to this volume is noted $N_{\gamma\,inter}$
588 The volume *V* corresponds to points a, b, c, d, e, f shown in Fig.18 is equal to:

$$V = V_T - 2\left(\frac{1}{2}V_4\right) - 4\left(\frac{1}{2}V_5\right) = V_T - V_4 - 2V_5 \quad (40)$$

589 Where V_T is the total volume of soil located within the failure mechanism for an

590 isolated square anchor plate.

591 Using Equations (31 and 33), we obtain:

$$V = B^2H + H^2B\tan\theta - \frac{1}{4}BS^2\cot\theta + BSH - SH^2\tan\theta + \frac{1}{12}S^3\cot\theta - \frac{1}{2}S^2H \quad (41)$$

592 The ultimate pullout capacity of one anchor plate located between two anchor plates

593 is given by:

$$q_{u\ inter} = \frac{Q_{u\ inter}}{A} = \frac{Q_{u\ inter}}{B^2} = \frac{\gamma \times V}{B^2} \quad (42)$$

$$q_{u\ inter} = \gamma H\left(1 + \left(\frac{H}{B}\right)\tan\theta - \frac{1}{4}\left(\frac{S}{B}\right)\left(\frac{S}{H}\right)\cot\theta + \frac{S}{B} + \left(\frac{S}{B}\right)\left(\frac{H}{B}\right)\tan\theta + \frac{1}{12}\left(\frac{S}{B}\right)^2\left(\frac{S}{H}\right)\cot\theta - \frac{1}{2}\left(\frac{S}{B}\right)^2\right) \quad (43)$$

594 Since:

$$\boldsymbol{q_{u\ inter} = \gamma H N_{\gamma\ inter}} \quad (44)$$

595 We get:

$$\boldsymbol{N_{\gamma\ inter} = 1 + \left(1 + \frac{S}{B}\right)\frac{H}{B}\tan\theta - \frac{1}{3}\frac{S}{B}\frac{S}{H}\left(\frac{1}{4}\frac{S}{B} - 1\right)\cot\theta - \frac{1}{2}\left(\frac{S}{B}\right)^2 + \frac{S}{B}} \quad (45)$$

596

597 **List of figures captions**:

598 Fig. 1 Geometrical model of group of four square anchor plates

599 Fig. 2 Total displacements for an isolated square anchor plate (*H/B*=4)

600 Fig. 3 Influence of Young's modulus on the pullout load for an isolated plate (H/B = 4,

601 H/B = 6)

602 Fig. 4 Group of square anchor plates in row configuration

603 Fig. 5 The ultimate pullout load versus displacement for two anchor plates with

604 varying spacing and an isolated anchor plate

605 Fig. 6 Deformed mesh for two anchor plates, *H/B* = 2 and *S/B* = 2
606 Fig. 7 Group efficiency of square anchor plates in row configuration
607 Fig. 8 Group of square anchor plates in square configuration
608 Fig. 9 Total displacements for nine (3 x 3) anchor plates in square configuration, *H/B*
609 = 4 and *S/B* = 2
610 Fig. 10 Group efficiency for four and nine plates in square configuration
611 Fig. 11 Load factor of group of square plates in row configuration
612 Fig. 12 Load factor of group of square plates in square configuration
613 Fig. 13 Influence of installation depth on the group efficiency
614 Fig. 14 Total displacements for a group of two plates with *H/B* = 4 ; 6 ; 8 and 10
615 Fig. 15 Influence of internal friction angle of soil on the group efficiency
616 Fig. 16 Influence of dilation angle on the group efficiency
617 Fig. 17 Influence of anchor roughness on the group efficiency
618 Fig. 18 Modified failure mechanism
619 Fig. 19 Break-out factor for square anchor plate in cohesionless soil
620 Fig. 20 Comparison of analytical and numerical Break-out factor for square anchor
621 plate (B=1m) in cohesionless soil
622 Fig. 21 Interference of two anchor plates: (a) 3D view, (b) Cross section A-A'
623 Fig. 22 Numerical, analytical and experimental comparison of group efficiency of two
624 square anchor plates
625 Fig. 23 Interference of *n* square anchor plates: (a) 3D view, (b) Cross section A-A'
626 Fig. 24 Comparison of numerical, analytical and experimental results of group
627 efficiency of five square plates in row configuration
628 Fig. 25 Failure mechanism for isolated square plate
629 Fig. 26 Interference detail of two failure mechanisms

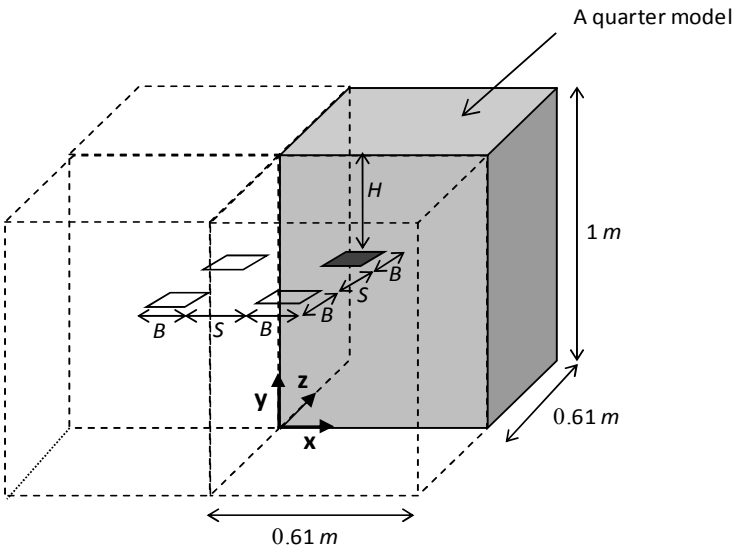


Fig. 1

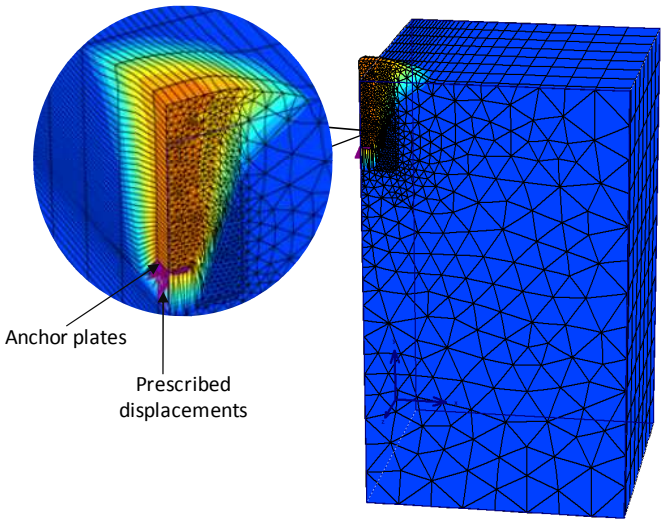


Fig. 2

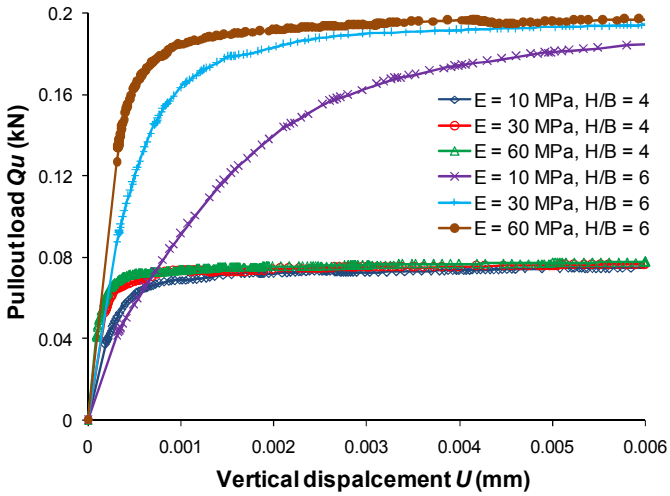

0.2
0.16
0.12
0.08
0.04
0
Pulloutload Qu (kN)
0
0.001
0.002
0.003
0.004
0.005
0.006
Vertical dispalcement U (mm)
E = 10 MPa, H/B = 4
E = 30 MPa, H/B = 4
E = 60 MPa, H/B = 4
E = 10 MPa, H/B = 6
E = 30 MPa, H/B = 6
E = 60 MPa, H/B = 6

Fig. 3

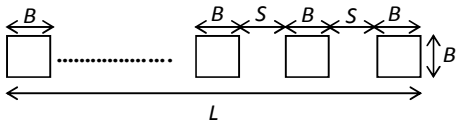


Fig. 4

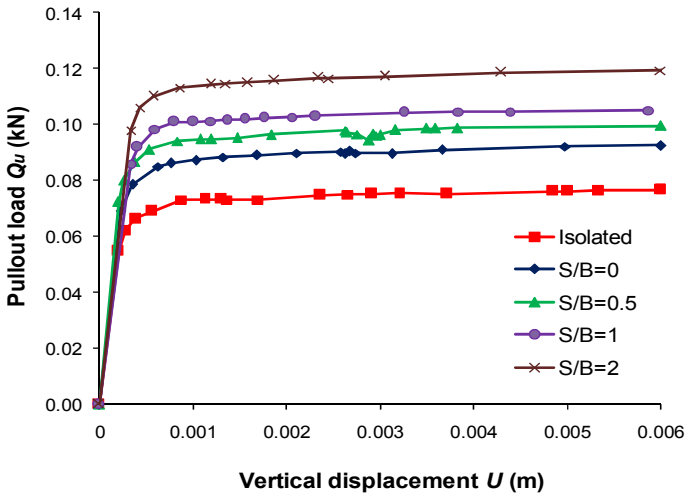

0.14
0.12
0.10
0.08
0.06
0.04
0.02
0.00
Pullout load Qu (kN)
0
0.001
0.002
0.003
0.004
0.005
0.006
Vertical displacement U (m)
Isolated
S/B=0
S/B=0.5
S/B=1
S/B=2

Fig. 5

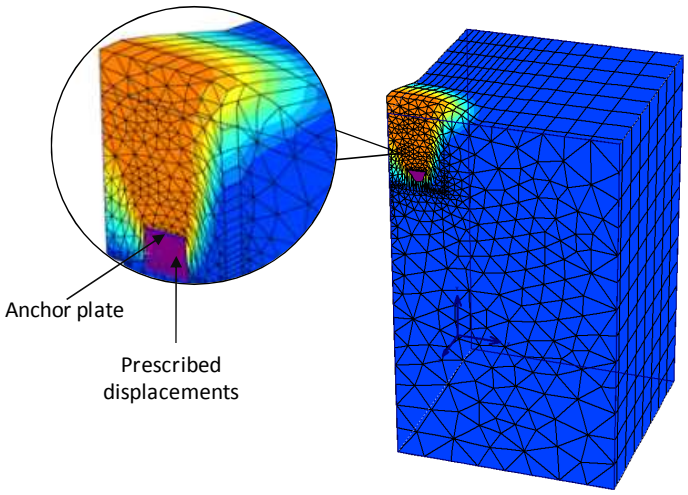


Fig. 6

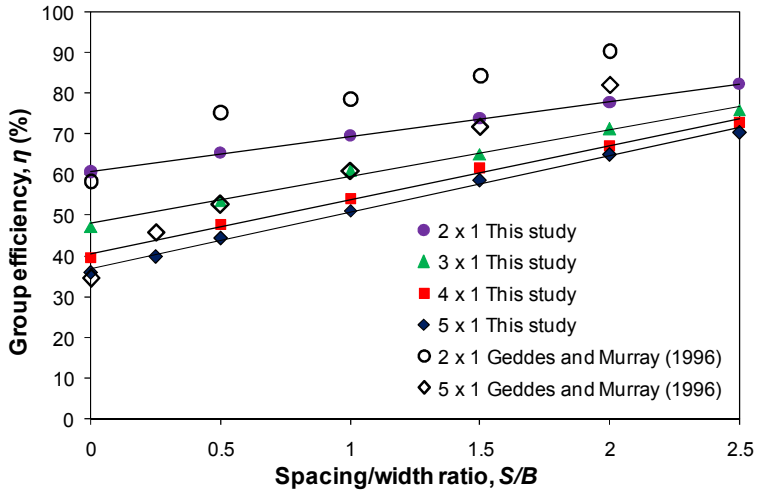

100
90
80
70
60
50
40
30
20
10
0
0
0.5
1
1.5
2
2.5
Group efficiency, η (%)
Spacing/width ratio, S/B
2 x 1 This study
3 x 1 This study
4 x 1 This study
5 x 1 This study
2 x 1 Geddes and Murray (1996)
5 x 1 Geddes and Murray (1996)

Fig. 7

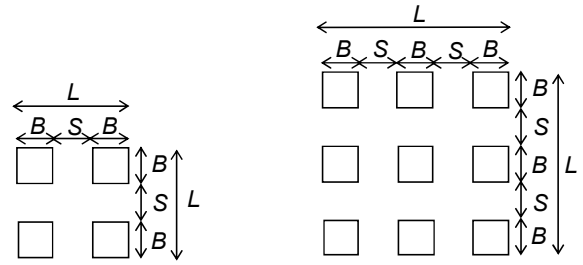


Fig. 8

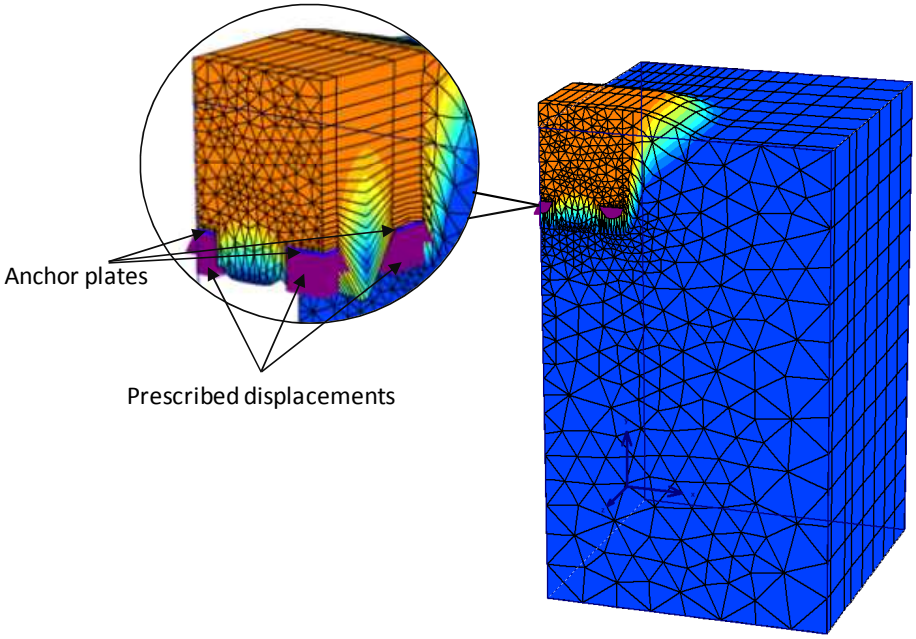


Fig. 9

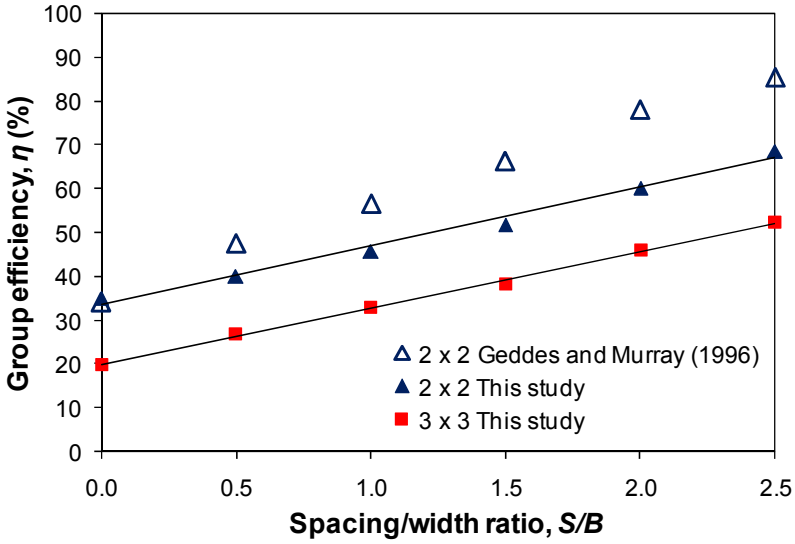

Group efficiency, η (%)
100
90
80
70
60
50
40
30
20
10
0
0.0
0.5
1.0
1.5
2.0
2.5
Spacing/width ratio, S/B
2 x 2 Geddes and Murray (1996)
2 x 2 This study
3 x 3 This study

Fig. 10

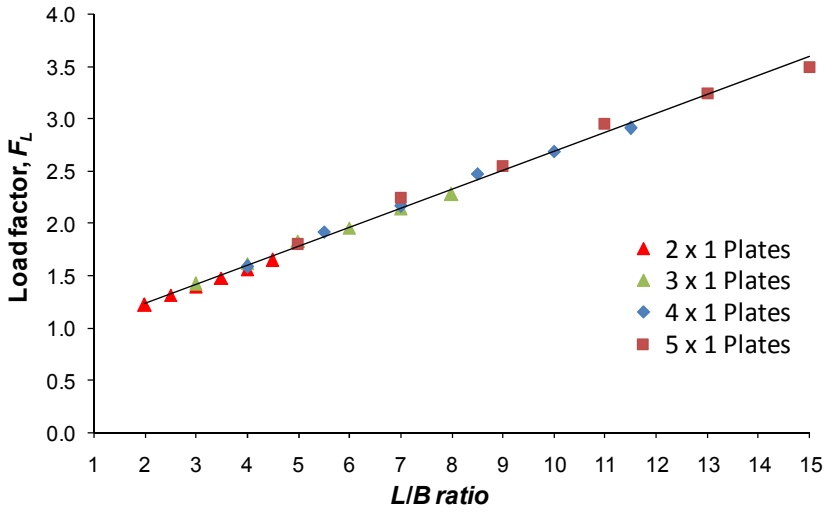

Load factor, F_L
4.0
3.5
3.0
2.5
2.0
1.5
1.0
0.5
0.0
1
2
3
4
5
6
7
8
9
10
11
12
13
14
15
L/B ratio
2 x 1 Plates
3 x 1 Plates
4 x 1 Plates
5 x 1 Plates

Fig. 11

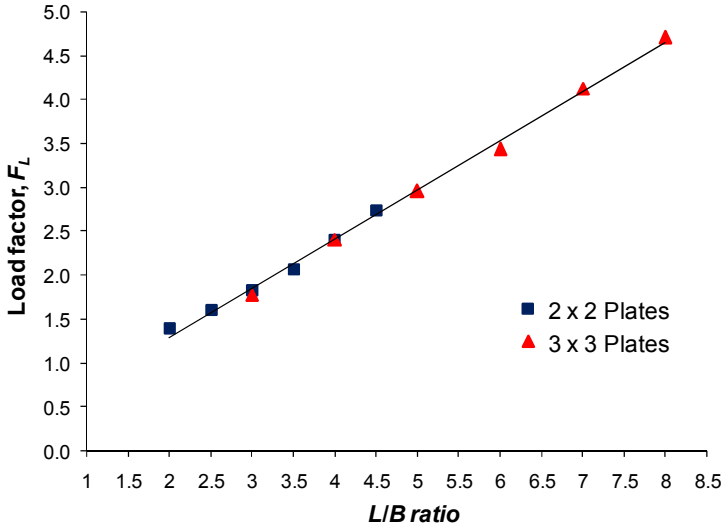

Load factor, F_L
5.0
4.5
4.0
3.5
3.0
2.5
2.0
1.5
1.0
0.5
0.0
1
1.5
2
2.5
3
3.5
4
4.5
5
5.5
6
6.5
7
7.5
8
8.5
L/B ratio
2 x 2 Plates
3 x 3 Plates

Fig. 12

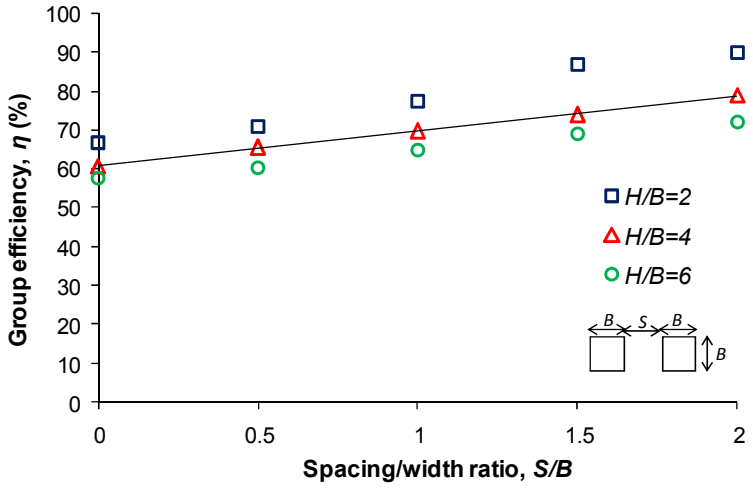

Group efficiency, η (%)
100
90
80
70
60
50
40
30
20
10
0
0
0.5
1
1.5
2
Spacing/width ratio, S/B
H/B=2
H/B=4
H/B=6
B
S
B
B

Fig. 13

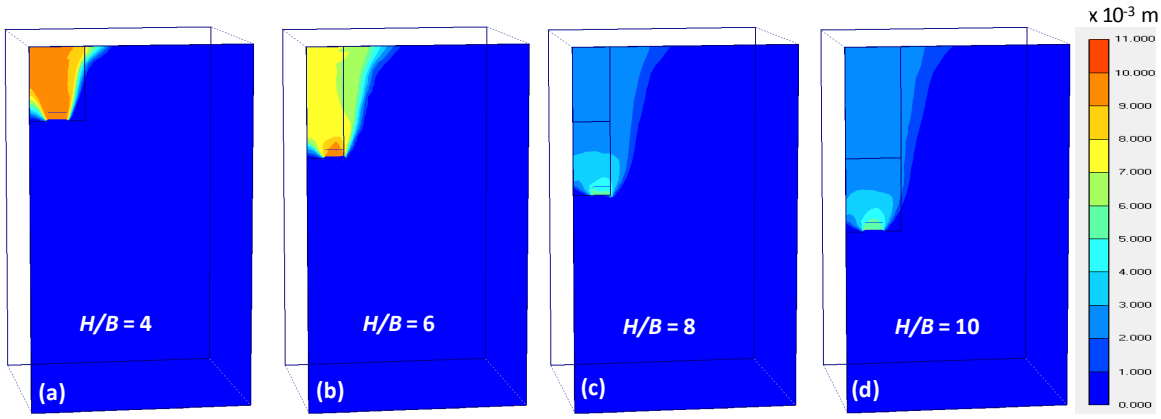

x 10-3 m
11.000
10.000
9.000
8.000
7.000
6.000
5.000
4.000
3.000
2.000
1.000
0.000
H/B = 4
(a)
H/B = 6
(b)
H/B = 8
(c)
H/B = 10
(d)

Fig. 14

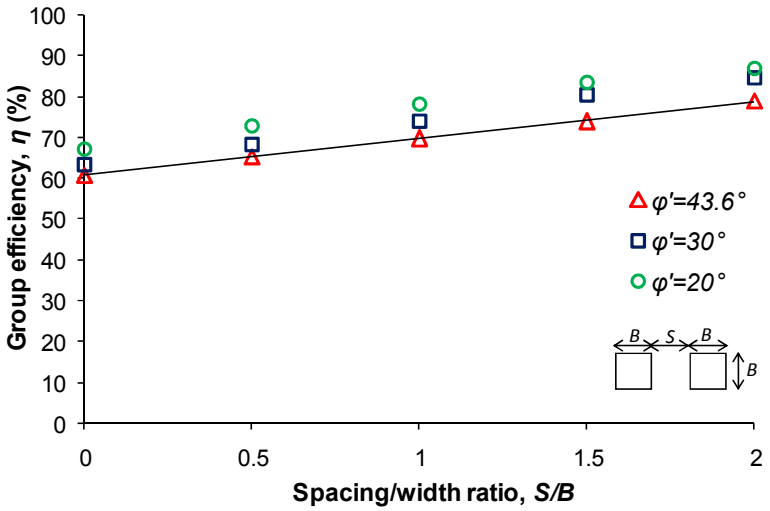

100
90
80
70
60
50
40
30
20
10
0
Group efficiency, η (%)
0
0.5
1
1.5
2
Spacing/width ratio, S/B
φ'=43.6°
φ'=30°
φ'=20°
B
S
B
B

Fig. 15

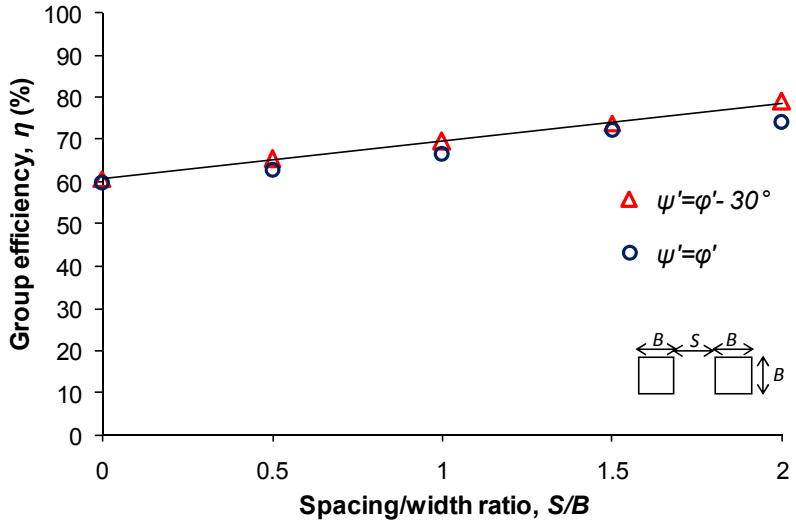

Group efficiency, η (%)
100
90
80
70
60
50
40
30
20
10
0
0
0.5
1
1.5
2
Spacing/width ratio, S/B
ψ′=φ′- 30°
ψ′=φ′
B
S
B
B

Fig. 16

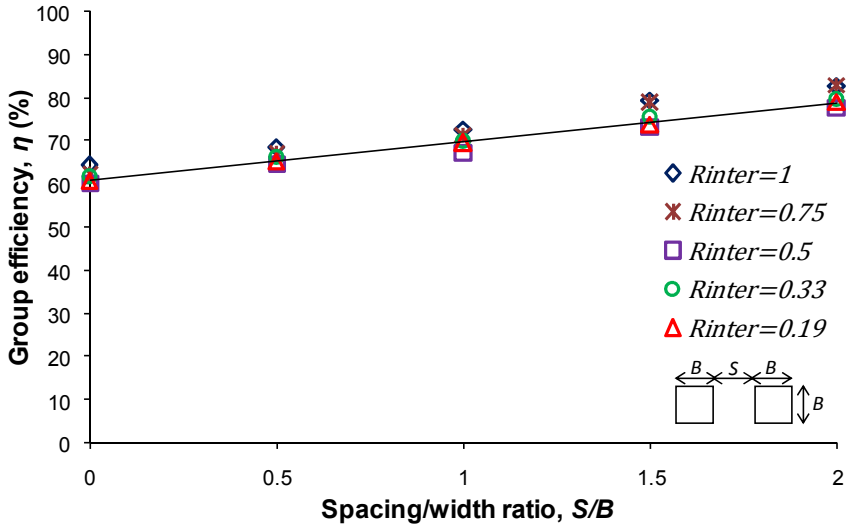

100
90
80
70
60
50
40
30
20
10
0
Group efficiency, η (%)
0
0.5
1
1.5
2
Spacing/width ratio, S/B
Rinter=1
Rinter=0.75
Rinter=0.5
Rinter=0.33
Rinter=0.19
B
S
B
B

Fig. 17

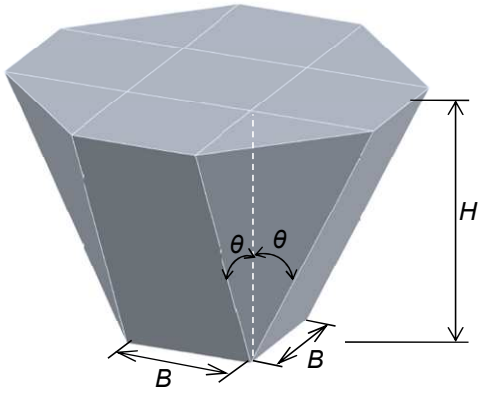


Fig. 18

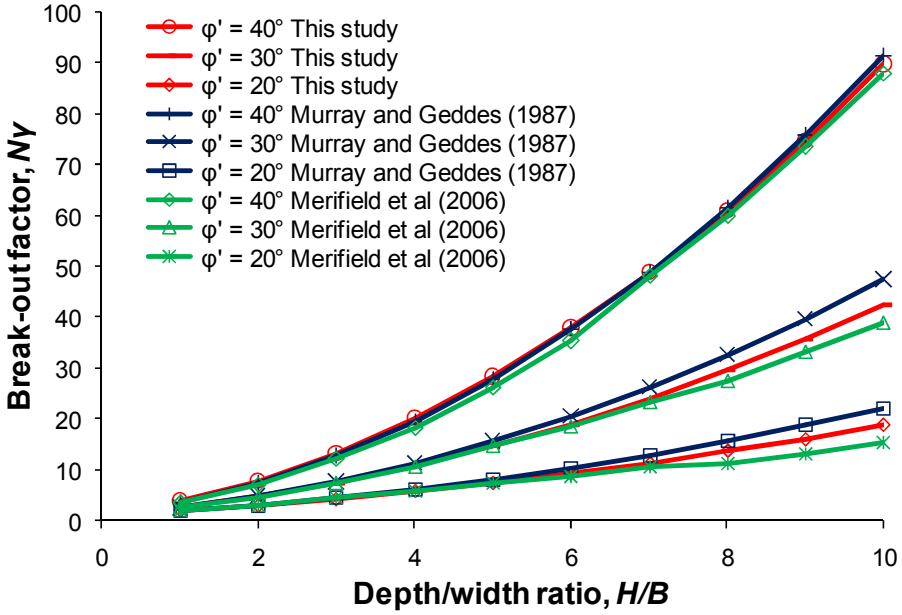

φ' = 40° This study
φ' = 30° This study
φ' = 20° This study
φ' = 40° Murray and Geddes (1987)
φ' = 30° Murray and Geddes (1987)
φ' = 20° Murray and Geddes (1987)
φ' = 40° Merifield et al (2006)
φ' = 30° Merifield et al (2006)
φ' = 20° Merifield et al (2006)
Break-out factor, Ny
Depth/width ratio, H/B
0
10
20
30
40
50
60
70
80
90
100
0
2
4
6
8
10

Fig. 19

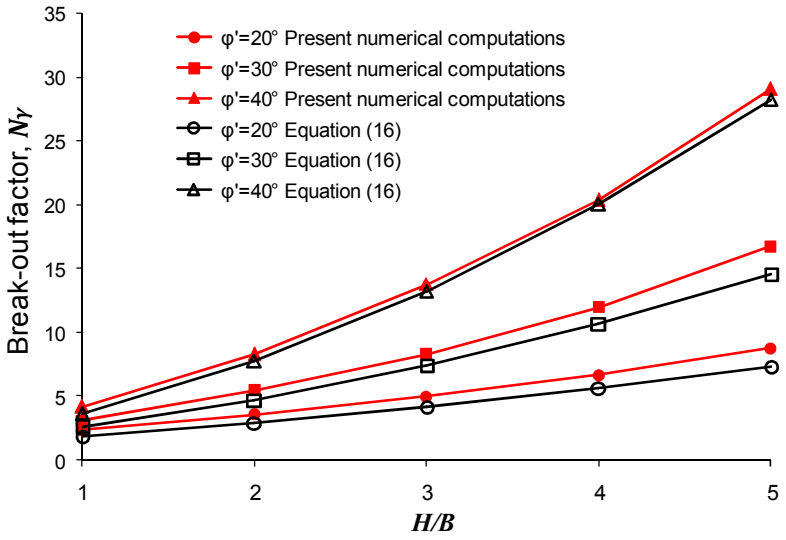

φ'=20° Present numerical computations
φ'=30° Present numerical computations
φ'=40° Present numerical computations
φ'=20° Equation (16)
φ'=30° Equation (16)
φ'=40° Equation (16)
Break-out factor, Nγ
H/B
0
5
10
15
20
25
30
35
1
2
3
4
5

Fig. 20

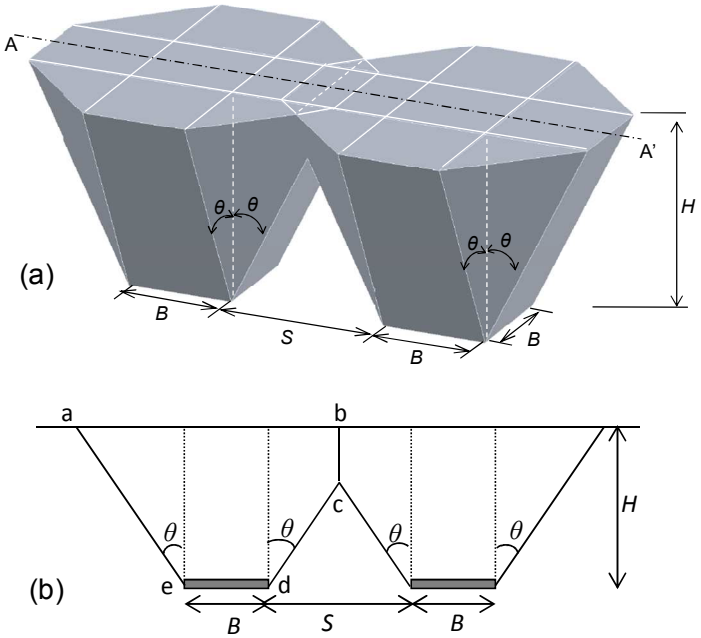


Fig. 21

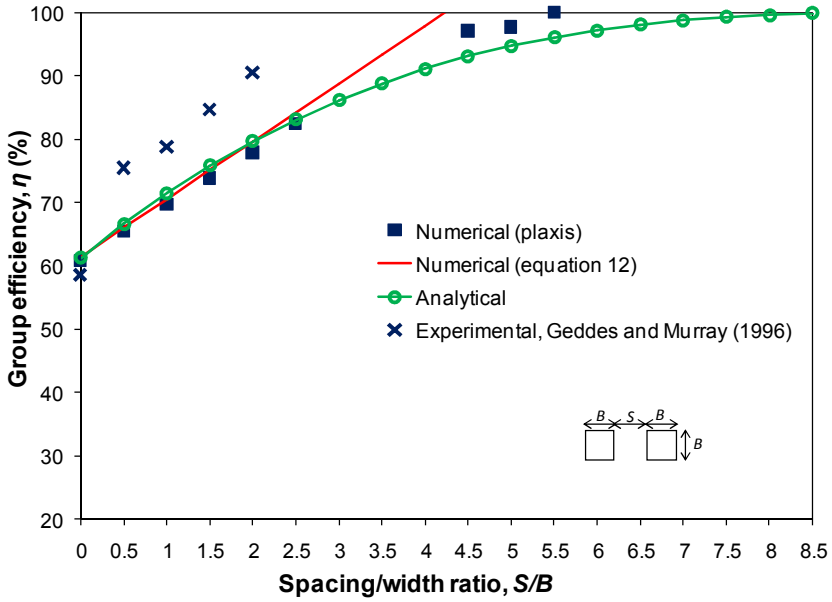

Group efficiency, η (%)
Spacing/width ratio, S/B
Numerical (plaxis)
Numerical (equation 12)
Analytical
Experimental, Geddes and Murray (1996)
B
S
B
B

Fig. 22

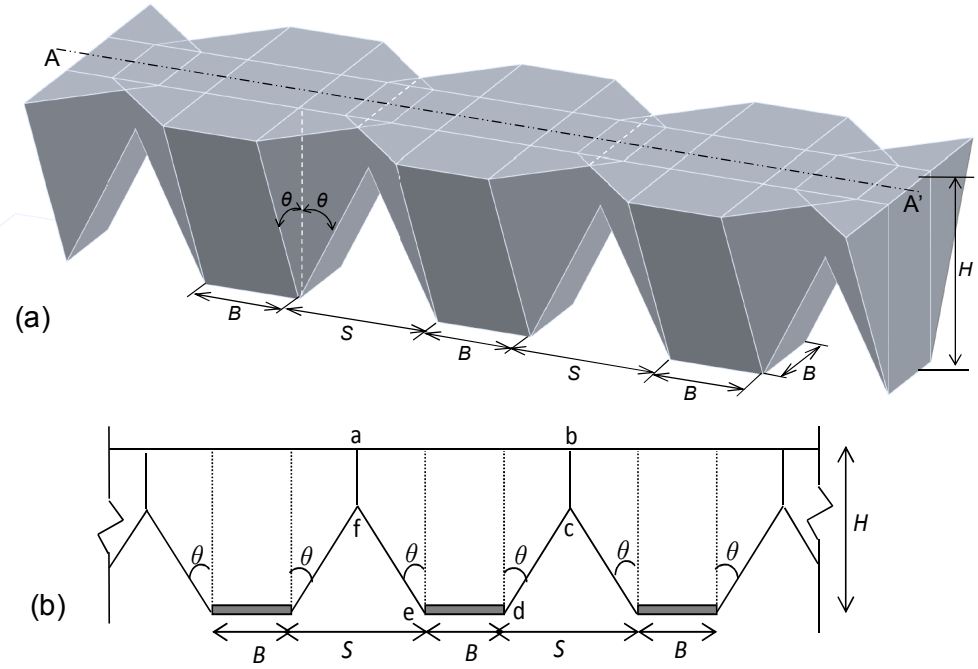


Fig. 23

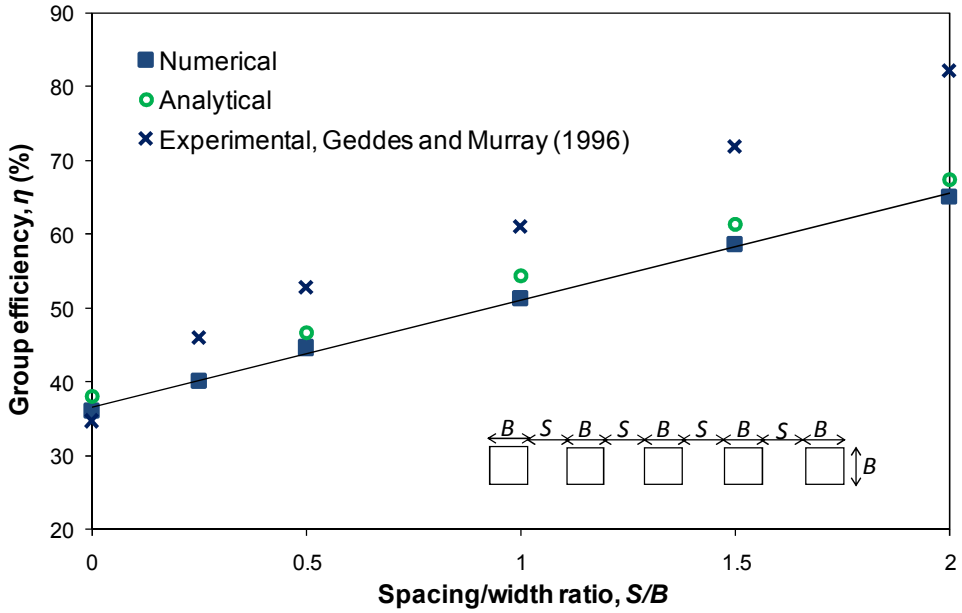

Numerical
Analytical
Experimental, Geddes and Murray (1996)
Group efficiency, η (%)
Spacing/width ratio, S/B
90
80
70
60
50
40
30
20
0
0.5
1
1.5
2
B
S
B
S
B
S
B
S
B
B

Fig. 24

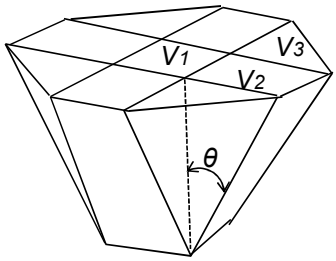


Fig. 25

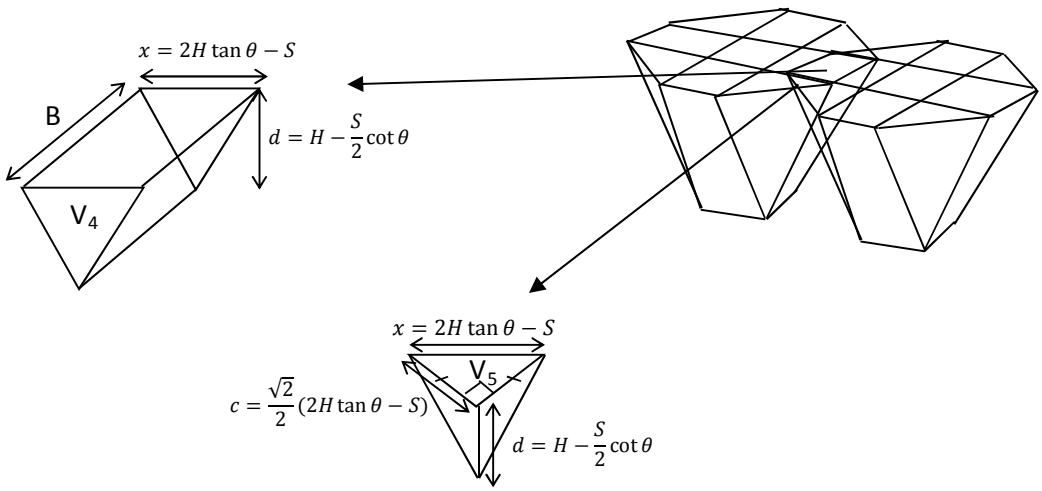

$x = 2H\tan\theta - S$
B
$d = H - \frac{S}{2}\cot\theta$
V_4
$x = 2H\tan\theta - S$
V_5
$c = \frac{\sqrt{2}}{2}(2H\tan\theta - S)$
$d = H - \frac{S}{2}\cot\theta$

Fig. 26